Amino Acids
https://doi.org/10.1007/s00726-019-02816-0

ORIGINAL ARTICLE

Synthesis, protonation constants and biological activity determination of amino acid–salicylaldehyde-derived Schiff bases

Claudia Fattuoni[1] · **Sarah Vascellari**[2] · **Tiziana Pivetta**[1]

Received: 24 September 2019 / Accepted: 27 December 2019

Abstract

Schiff bases represent a class of molecules widely studied for their importance in organic and coordination chemistry. Despite the large amount of studies on the chemical and biological properties of the Schiff bases, the different experimental conditions prevent a useful comparison to search for a correlation structure–activity. Moreover, literature is lacking in comprehensive data on the spectroscopic characterization of these compounds. For this reason, six Schiff bases, derived from salicylaldehyde and natural amino acids were fully characterized by nuclear magnetic resonance and infrared spectroscopy, and their aqueous solution equilibria, antiproliferative activity and DNA-binding activity were examined. All experimental conditions were kept constants to achieve comparable information and useful insights about their structure–activity correlation. The synthesized compounds showed DNA binding constants in the 10^1–10^2 M^{-1} range, depending on the substituent present in the amino acid side-chain, and resulted devoid of significant cytotoxic activity against the different human tumor cell lines showing IC50 values higher than 100 μM.

Keywords Schiff bases · L-Amino acids · DNA binding · Cytotoxicity · Aqueous solution equilibria

Introduction

Schiff bases, also known as imines or azomethines and named after their discoverer Hugo Schiff, are condensation products of primary amine and aldehydes or ketones (Qin et al. 2013). Schiff bases are important intermediates in bio-processes such as the transamination reaction or the protein glycation and are involved in racemization and decarboxylation reactions (Vilanova et al. 2012; El-Sherif and Aljahdali 2013; Rajesh and Ray 2014). In organic synthesis, Schiff bases are useful building blocks in addition, hetero Diels–Alder (Dossetter et al. 1999) and Staudinger (Palomo et al. 1999) reactions. The last is widely used for the preparation of β-lactams, a widely used class of antibiotics, by reaction of a Schiff base with ketenes (Turan et al. 2016). Other Schiff bases show biological activity against fungi and bacteria (Malik et al. 2018; Antony et al. 2019). In addition, some derivatives have been recently proposed for the treatment of Alzheimer's disease, as metal binding agents able to promote the disaggregation of amyloid-β plaques (Gomes et al. 2014). Thanks to their soft–hard donor character, Schiff bases are commonly used as ligands for several metal ions. They are used to recognize anions and cations and their application in biochemical and environmental fields has been proposed (Dalapati et al. 2014). Moreover, complexes formed by Schiff bases with metals such as Cu (II) (Qiao et al. 2011), Cd (II) (Zhang et al. 2012), Ru (II) (Chow et al. 2014), Zn (II) (Zhong et al. 2006) and lanthanides (Yang et al. 2000) show antitumor activity. Recently the applications of Schiff bases and their metal complexes in the field of chiral catalysis, functional materials and antitumor bioactive substances

Handling Editor: E. R. Perez Gonzalez.

Electronic supplementary material The online version of this article (https://doi.org/10.1007/s00726-019-02816-0) contains supplementary material, which is available to authorized users.

✉ Claudia Fattuoni
cfattuon@unica.it

✉ Tiziana Pivetta
tpivetta@unica.it

[1] Department of Chemical and Geological Sciences, University of Cagliari, Cittadella Universitaria, Monserrato, 09042 Cagliari, Italy

[2] Department of Biomedical Sciences, University of Cagliari, Cittadella Universitaria, Monserrato, 09042 Cagliari, Italy

Published online: 13 January 2020

have been reviewed (Pessoa and Mannar 2017; Liu et al. 2018; Banti et al. 2019). The potential development of pharmaceutical applications of these compounds requires a proper knowledge of their chemical and biological reactions and also of their toxicological profile. Despite the high level of interest in the scientific community for these molecules, a literature survey highlighted a general lack of consistency. In fact, although Schiff bases have been widely studied under different points of view, a direct comparison of the reported data is not possible because of the different experimental conditions. This problem is relevant for the aqueous solution equilibria study, since protonation constants of Schiff bases belonging to the same family are often determined in different solvents, temperatures, and ionic buffers (el Sherif and Aljahdali 2013; Galić et al. 1997; Metzler et al. 1980; Turkoglu et al. 2011). Due to the fundamental importance of the protonation constants in the study of the complex formation, it appears necessary that all experiments are carried out in the same conditions at least for homologous series of compounds. Another discrepancy in the literature data is the lack of nuclear magnetic resonance (NMR) characterization of several amino acid derived Schiff bases: in some case only the melting point was reported, or only the ^{1}H-NMR chemical shift data. Some molecules have never been characterized, such as the salicylaldehyde/serine or histidine derivatives. Moreover, some reported data are incomplete or inconsistent. For the above reported considerations, we decided to synthesize six Schiff bases from salicylaldehyde and proteinogenic L-amino acids, and to study their properties in the same experimental conditions to have comparable information on their chemical and biological behavior. In particular, we studied the aqueous solution equilibria, the cytotoxic activity and the DNA binding ability of L-salicylidenealanine, *N*-[(2-hydroxyphenyl)methylene]-L-alanine (**1a**), L-salicylidenevaline *N*-[(2-hydroxyphenyl)methylene]-L-valine (**1b**), L-salicylidenecysteine *N*-[(2-hydroxyphenyl)methylene]-L-cysteine (**1c**), L-salicylideneserine *N*-[(2-hydroxyphenyl)methylene]-L-Serine (**1d**), L-salicylidenearginine *N*-[(2-hydroxyphenyl)methylene]-L-arginine (**1e**), and L-salicylidenehistidine *N*-[(2-hydroxyphenyl)methylene]-L-histidine (**1f**) (Scheme 1). The chosen compounds were prepared modifying literature methods, to improve the product yield. All compounds were fully characterized by elemental analysis, NMR (^{1}H- and ^{13}C-NMR) and Infrared (IR) spectroscopy techniques. The protonation constants of the compounds were determined by potentiometric and spectrophotometric titrations, carried out simultaneously in aqueous solution at 25 °C in 0.1 M ionic strength (NaCl). The interaction of **1a–f** bases with calf thymus DNA (ct-DNA) and the cytotoxic activity against a panel of human tumor cell lines (SK-MES-1, DU-145, Hep-G2, CCRF-CEM, CCRF-SB) were also examined.

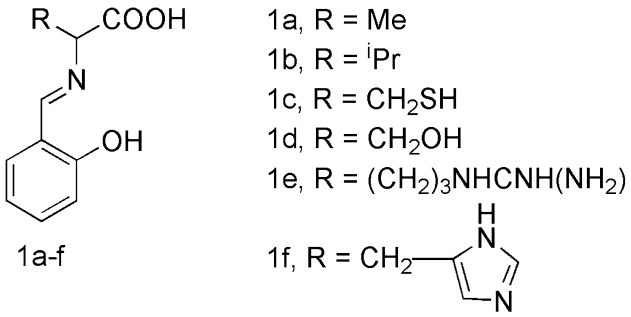

Scheme 1 Schiff bases synthesized from salicylaldehyde and amino acids L-alanine (a), L-valine (b), L-cysteine (c), L-serine (d), L-arginine (e), L-histidine (f)

Experimental

Calf thymus DNA sodium salt, hydrochloric acid standard solutions, diethyl ether, dimethylsulfoxide-d6 (DMSO-d6), ethanol, L-alanine, L-arginine, L-cysteine, L-histidine, L-serine, L-valine, methanol, 1,4-piperazinediethanesulfonic acid (PIPES), potassium bromide, salicylaldehyde, sodium bromide, sodium chloride, sodium hydroxide pellets, sodium hydroxide standard solution and sodium sulfate were purchased from Sigma-Aldrich and used without any further purification. Infrared spectra of the studied compounds were recorded using a Bruker Equinox 55 spectrophotometer, in KBr medium (pellets). ^{1}H and ^{13}C NMR spectra were recorded on Varian 400 and 500 spectrometers. Proton and carbon chemical shifts in DMSO-d_6 were referenced to the residual solvent signals (^{1}H NMR, $\delta = 2.60$ ppm; ^{13}C NMR, $\delta = 39.6$ ppm). Melting points (mp) were measured using a Kofler hot stage microscope and are uncorrected.

Synthesis of L-salicylideneaniline (1a)

Compound **1a** was prepared according to a literature method (Hsieh et al. 2007). A mixture of L-alanine (0.8 g, 9 mmol), salicylaldehyde (1 mL, 9 mmol) and Na_2SO_4 (4 g) in methanol (150 mL) was stirred under reflux for 12 h. The solid was filtered, and the solvent was removed under reduced pressure to give 1.6 g (90% yield) of light brown solid, mp 138–142 °C (dec). ^{1}H NMR (400 MHz, DMSO-d_6): δ 8.59 (s, 1H, CH=N), 7.46 (m, 1H, Ar–H), 7.35 (m, 1H, Ar–H), 6.90 (m, 2H, Ar–H), 4.21 (q, 1H, CH–CO_2H, $J = 6.7$), 1.44 (d, 3H, CH_3, $J = 6.7$). ^{13}C NMR (125 MHz, DMSO-d_6): δ 19.48, 64.79, 116.60, 117.36, 118.69, 131.93, 132.69, 160.62, 166.61, 173.29. IR (KBr): ν/cm^{-1} 3418, 3090, 2604, 1630, 1595, 1452, 1409, 1356, 1309, 1117, 853, 542.

Elemental analysis found (calc. for $C_{10}H_{11}NO_3$): C% 61.80 (62.17), H% 5.64 (5.74), N% 7.21 (7.25).

Synthesis of L-salicylidenevaline (1b)

Compound **1b** was prepared as reported for **1a** to give 1.22 g (62% yield) of light yellow solid, mp 162–164 °C. ^{1}H NMR (500 MHz, DMSO-d_6): δ 0.89 (d, 3H, CH_3, J = 4 Hz), 0.91 (d, 3H, CH_3, J = 4.5 Hz), 2.26 (m, 1H, CH–CH_3), 3.82 (m, 1H, CH–CO_2H), 6.89 (m, 2H, Ar–H), 7.35 (t, 1H, Ar–H, J = 7.6 Hz), 7.45 (d, 1H, Ar–H, J = 7.6 Hz), 8.53 (s, 1H, CH=N). ^{13}C NMR (100 MHz, DMSO-d_6): δ 17.8, 19.3, 31.1, 75.9, 116.6, 118.6, 118.7, 132.0, 132.7, 160.8, 167.4, 172.4. IR (KBr): ν/cm^{-1} 3430, 2961, 2626, 1648, 1589, 1511, 1394, 1330, 757, 541. Elemental analysis found (calc. for $C_{12}H_{15}NO_3$): C% 64.98 (65.14), H% 6.84 (6.83), N% 6.21 (6.33).

Synthesis of L-salicylidenecysteine (1c)

A mixture of L-cysteine (1.09 g, 9 mmol) and salicylaldehyde (1 mL, 9 mmol) in ethanol (50 mL) was stirred under reflux for 12 h (Pillai et al. 1999). The solid product was filtered, washed with ethanol and dried. The white solid obtained (1.75 g, 86% yield) showed in the NMR analysis to be formed by two isomers (*E* and *Z*) of compound **1c**, mp 166–167 °C. ^{1}H NMR (500 MHz, DMSO-d_6): δ (*E*) 2.97 (dd unresolved, 1H, CH_2, J = 9.5 Hz), 3.34 (dd, 1H, CH_2, J = 7 and 9.5 Hz), 4.20 (m, 1H, CH–CO_2H), 5.65 (s, 1H, CH=N), 6.81 (t, 2H, Ar–H, J = 7 Hz), 7.13 (t, 1H, Ar–H, J = 7.5 Hz), 7.34 (d, 1H, Ar–H, J = 7 Hz); δ (*Z*) 3.03 (dd, 1H, CH_2, J = 5 and 10 Hz), 3.20 (dd, 1H, CH_2, J = 7 and 10 Hz), 3.82 (m, 1H, CH–CO_2H), 5.85 (s, 1H, CH=N), 6.76 (m, 2H, Ar–H), 7.06 (t, 1H, Ar–H, J = 7.5 Hz), 7.30 (d, 1H, Ar–H, J = 7.5 Hz). ^{13}C NMR (100 MHz, DMSO-d_6): δ (*E*) 37.11 (CH_2), 64.85 (CH–C=O), 65.69 (CH=N), 115.15 ($C_{Ar–H}$), 118.81 ($C_{Ar–H}$), 127.67 ($C_{Ar–C}$), 126.16 ($C_{Ar–H}$), 128.16 ($C_{Ar–H}$), 155.23 ($C_{Ar–OH}$), 172.98 (C=O); δ (*Z*) 38.21 (CH_2), 65.26 (CH–C=O), 67.73 (CH=N), 115.74 ($C_{Ar–H}$), 119.10 ($C_{Ar–H}$), 124.30 ($C_{Ar–C}$), 127.94 ($C_{Ar–H}$), 129.09 ($C_{Ar–H}$),154.65 ($C_{Ar–OH}$),172.51 (C=O). IR (KBr): ν/cm^{-1} 3438, 3100, 2701, 2578, 1622, 1598, 1577, 1457, 1384, 1334, 1283, 760, 679. Elemental analysis found (calc. for $C_{10}H_{11}NO_3S$): C% 53.64 (53.32), H% 5.06 (4.92), N% 6.31 (6.22), S% 13.87 (14.23).

Synthesis of L-salicylideneserine (1d)

A mixture of L-serine (0.95 g, 9 mmol) and salicylaldehyde (1 mL, 9 mmol) in ethanol (50 mL) was stirred under reflux for 2.5 h, then kept in the refrigerator overnight. The solid product was filtered, washed with ethanol, and dried. Product **1d** was obtained as a light brown solid (1.00 g, 53% yield), mp 220 °C (dec). ^{1}H NMR (500 MHz, DMSO-d_6): δ 3.69 (dd, 1H, CH_2, J = 7.5 and 11 Hz), 3.86 (dd, 1H, CH_2, J = 4 and 11 Hz), 4.09 (dd, 1H, CH–CO_2H, J = 4 and 7.5 Hz), 6.90 (m, 2H, Ar–H), 7.35 (t, 1H, Ar–H, J = 7.5 Hz), 7.46 (d, 1H, Ar–H, J = 7.5 Hz), 8.53 (s, 1H, CH=N). ^{13}C NMR (125 MHz, DMSO-d_6): δ 62.7, 72.5, 116.7, 118.5, 118.7, 132.0, 132.7, 160.9, 167.6, 171.4. IR (KBr): ν/cm^{-1} 3444, 3054, 2947, 1635, 1618, 1603, 1507, 1472, 1416, 1348, 1313, 1125, 1015, 615, 527. Elemental analysis found (calc. for $C_{10}H_{11}NO_4$): C% 57.46 (57.41), H% 5.25 (5.30), N% 6.31 (6.70).

Synthesis of L-salicylidenearginine (1e)

Compound **1e** was prepared as reported for **1c** to give a bright yellow solid (2.45 g, 98% yield), mp 200–202 °C. ^{1}H NMR (500 MHz, DMSO-d_6): δ 1.58 (m, 2H, $CH_2C\mathit{H}_2CH_2$), 1.83 (m, 1H, $CHC\mathit{H}_2$), 2.01 (m, 1H, CH–CH_2), 3.18 (m, 2H, CH_2–NH), 3.88 (m, 1H, CH–COOH), 6.86 (m, 2H, Ar–H), 7.36 (t, 1H, Ar–H, J = 8 Hz), 7.45 (d, 1H, Ar–H, J = 8 Hz), 8.52 (s, 1H, CH=N), 9.60 (s, broad, 1H, NH). ^{13}C NMR (100 MHz, DMSO-d_6): δ 26.0, 31.6, 41.4, 71.3, 117.4, 118.2, 119.4, 133.2, 134.5, 157.5 (NH_2-C = NH), 165.3, 166.8, 174.8. IR (KBr): ν/cm^{-1} 3407, 3315, 3078, 2965, 2865, 1662, 1650, 1634, 1591, 1474, 1377, 1343, 1192, 1149, 777, 536. Elemental analysis found (calc. for $C_{13}H_{18}N_4O_3$): C% 56.16 (56.10), H% 6.59 (6.52), N% 20.08 (20.13).

Synthesis of L-salicylidenehistidine (1f)

A mixture of L-histidine (0.7 g, 4.5 mmol) and salicylaldehyde (1 mL, 9 mmol) in ethanol (50 mL) was stirred under reflux for 24 h. The solid product was filtered, washed with ethanol and dried. Product **1f** was obtained as a bright yellow solid (0.9 g, 77% yield), mp 174–180 °C. ^{1}H NMR (400 MHz, DMSO-d_6): δ 3.00 (dd, 1H, CH_2, J = 8.4 and 14.6 Hz), 3.18 (dd, 1H, CH_2, J = 4.8 and 14.6 Hz), 4.32 (dd, 1H, CH-CO_2H, J = 4.8 and 8.4 Hz), 6.77 (s, 1H, C=CH–N), 6.85 (m, 2H, Ar–H), 7.34 (m, 2H, Ar–H), 7.59 (s, 1H, NH–CH=N), 8.32 (s, 1H, CH=N). ^{13}C NMR (125 MHz, DMSO-d_6): δ 31.22, 70.19, 116.57, 118.59, 119.49, 129.28, 131.86, 132.63, 134.84, 136.46, 160.62, 166.93, 172.38. IR (KBr): ν/cm^{-1} 3422, 3122, 3018, 2879, 1638, 1531, 1470, 1416, 1341, 1267, 1149, 838, 624, 535. Elemental analysis found (calc. for $C_{13}H_{13}N_3O_3$): C% 60.19 (60.22), H% 4.97 (5.05), N% 16.24 (16.21).

Potentiometric and spectrophotometric titrations

Potentiometric titrations were carried out in a thermostated vessel with a Mettler-Toledo Seven Compact pH/Ion-meter, equipped with a Mettler-Toledo InLab Micro Pro combined

glass electrode with an integrated temperature probe. Potentiometric titrations were performed at 25 °C in 0.1 M ionic strength (NaCl) under N_2 atmosphere. The glass electrode was calibrated daily by titration of a known amount of HCl with carbonate-free NaOH standard solution. Electrode standard potential (E_0), water ionic product (pKw), electrode response and carbonate content of the titrant solution were checked with Gran's procedure (Gran 1952) using the Glee software (Gans and O'Sullivan 2000). The UV–Visible (UV–Vis) measurements were carried out with a Varian Cary 60 spectrometer equipped with an optical fiber dip probe with a 1 cm optical path length.

Protonation constants

Protonation constants of compounds **1a–f** were determined by spectrophotometric and potentiometric titrations, at 25 °C in 0.1 M ionic strength (NaCl), following the spectral variations due to the additions of the titrant. Solutions of ligand were prepared daily by dissolving the proper amount of the compound in freshly distilled water. Concentrations of compounds **1a–f** ranged from 2.8×10^{-4} to 1.0×10^{-3} M, according to their absorptivity and solubility. Solutions containing a known amount of compound and HCl (necessary to fully protonate the molecule) were titrated with NaOH standard solution. The reversibility of the involved equilibria was checked by back-titration with standard HCl. The overall stability constants were determined with the Hyperquad 2003 software (Gans et al. 1996).

DNA binding

The binding constants (Kb) between ct-DNA and compounds **1a–f** were determined at 25 °C by spectrophotometric titrations in PIPES buffer 0.01 M at pH 7.0. A stock solution of ct-DNA in 0.01 M PIPES buffer at pH 7.0 was prepared and stored at 4 °C. This solution was used within 4 days. The concentration of DNA per nucleotide was determined by UV absorption at 260 nm using its molar absorption coefficient (6600 M^{-1} cm^{-1}) (Reichmann et al. 1954). The purity of the DNA was checked by monitoring the ratio of the absorbance at 260 nm to that at 280 nm. A ratio higher than 1.8 indicates a DNA sufficiently protein-free (Murmur 1961). Twenty solutions containing a fixed amount of the compounds (ranging from $\approx 2.03 \times 10^{-4}$ to $\approx 6.07 \times 10^{-4}$ mmol, according to the absorptivity) and variable amounts of DNA (ranging from 6.09×10^{-4} to 1.82×10^{-3} mmol) were prepared. The stock solution of **1c** was prepared at least 39 h before the experiment due to its slow dissolution in PIPES. Since the interactions between DNA and compounds **1a–f** are slow processes, spectra in the 200–500 nm range were recorded when equilibration was reached (15 h). All solutions were stored in the dark at room temperature. The DNA binding constants were obtained by using the Hyperquad 2003 software (Gans et al. 1996).

Cell lines

Cell lines were purchased from the American Type Culture Collection (ATCC) and were derived from: lung squamous carcinoma (SK-MES-1, ATCC number HTB-SB); prostate carcinoma (DU-145, ATCC number HTB-B1); hepatocellular carcinoma (Hep-G2, ATCC number HB-8065); acute T-lymphoblastic leukemia (CCRF-CEM, CRL-8436); acute B-lymphoblastic leukemia (CCRF-SB, ATCC number CCL-120). All cell lines were grown at 37 °C in a 5% CO_2 atmosphere, in their specific media according to ATCC instructions, in the presence of 5–10% fetal bovine serum (FBS), antibiotic and, unless otherwise indicated, sodium pyruvate. All cell cultures were maintained in exponential growth by periodically splitting high density suspension cultures (i.e. 106 cell/mL) or when cell monolayers reached sub-confluence (70–90% confluence). The absence of mycoplasma contamination was checked periodically by the Hoechst staining method (Latt et al. 1975).

Cytotoxic assays

The cytotoxic effect of the compounds **1a–f** was evaluated in cell lines during the exponential growth stage. Stock solutions of **1a–f** were stored at 4 °C in the dark. For the evaluation of cytotoxicity, solutions of compounds **1a–f** were serially diluted in growth medium specific for the different cell lines. Suspension cell lines were seeded in 96-well plates at an initial density of 1×10^5 cells/mL in specific growth medium, with or without serial dilutions of each compound. Adherent cell lines were seeded at an initial density of 1×10^4 cells per well and incubated overnight before adding serial dilutions of the test compound. Cell viability was determined after 96 h at 37 °C, 5% CO_2, by the 3-(4,5-dimethylthiazol-2-yl)-2,5-diphenyl-tetrazolium bromide (MTT) method as previously described (Pauwels et al. 1988). Cell growth at each drug concentration was expressed as the percentage of untreated controls. The results were expressed as IC50, i.e. the concentration of compound required to reduce the viability of the tested cells by 50%. The antitumor agent vincristine was used as a reference compound.

Results and discussion

Literature reports many different synthetic methods to prepare amino acid-derived Schiff bases (Smith et al. 1977; Rao and Philipp 1991; Saleem et al. 2012; Ershov et al. 2013). The classic method to synthesize Schiff bases consists of

simply mixing equimolar amounts of amine and aldehyde in ethanol and refluxing the mixture for some hours: the desired product readily formed can be filtered and isolated. When the amine role is played by an α-amino acid, the synthetic procedure may not be so straightforward, due to the amino acid zwitterionic character resulting in a weakly nucleophilic amino group. Several modifications of the classic method have been reported. For example, potassium (Liu et al. 2012) or sodium hydroxide (Hiskey and Jung 1963) was added to an aqueous or methanolic solution of the amino acid to enhance its nucleophilic character. An analogous effect is obtained with a bicarbonate buffer (Rao and Philipp 1991). On the other hand, the added base has the effect of promoting the aldehyde self-reaction, leading to a lower yield of the desired Schiff base. We found that the simple mixing-reflux method can be applied only to cysteine and arginine. To obtain a satisfactory yield from the other four amino acids, the classic method must be modified as follows: (i) for the histidine derivative, a double amount of aldehyde was used; (ii) for alanine and valine derivatives, anhydrous sodium sulfate was added to the reaction mixture as reported by Hsieh (Hsieh et al. 2007); (iii) for serine derivative, an equimolar mixture of amino acid and aldehyde was refluxed in ethanol for 2 h and the resulting solution was kept in the refrigerator overnight. The high reactivity of cysteine in the reported condition is noteworthy: in fact, after only 1 h at the reflux temperature a thick white precipitate was obtained. The NMR analysis revealed that it constituted by two geometric isomers E and Z. The E isomer was the more abundant, due to the lower steric hindrance: the correspondence of the imino CH=N proton chemical shift value with those reported (Maurya et al. 2008) allows its identification. All attempts to prepare only one isomer, lowering the reaction temperature or increasing the solvent amount, were unsuccessful.

The protonation constants were determined by a basic titration, measuring simultaneously the electrochemical potential and the UV–Vis absorption. The absorbance values measured during the potentiometric titrations of **1a** and **1b** are reported vs wavelength and pH in Fig. 1 as an example. Spectra recorded during the titrations of the other compounds are reported in the Supporting material. The functional groups involved in the protonation and the protonation sequence were determined by comparing the pure UV–Vis spectra of the formed species. No reliable NMR spectra in water solution were obtained due to the low water solubility of the compounds (< 1 mM).

Spectral evidences

By titrating the synthesized compounds, several equilibria were spectrally evidenced in the 2–11.4 pH range: three for

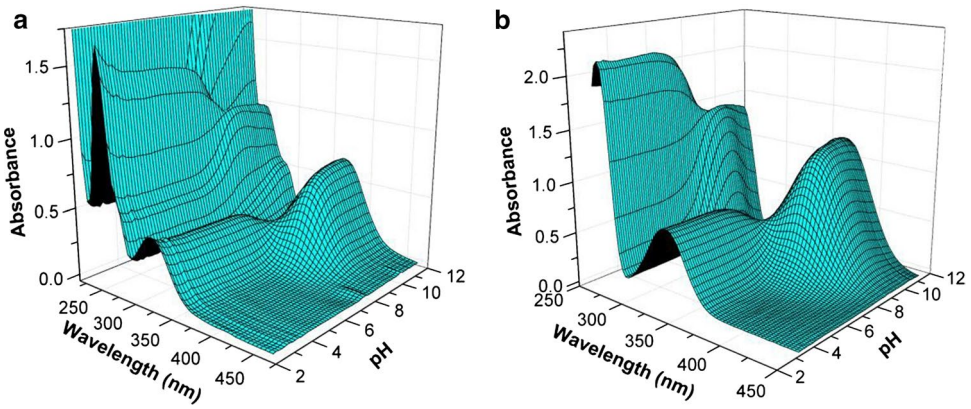

Fig. 1 Absorbance as a function of wavelength and pH measured during the titrations of 0.0240 mmol of **1a** (**a**) and 0.0178 mmol of **1b** (**b**); 25 °C, 0.1 M NaCl ionic buffer, 1 cm optic path length. Compound **1a**: by titrating compound **1a** with NaOH, three equilibria are spectrally evidenced in the pH range 2–11.4 (Fig. S1). At pH 2, two peaks and a shoulder are present at 325, 257 and ≈ 280 nm, respectively. Increasing the pH, the absorbance of the peaks slightly decreases, not for the dilution as can be seen in the inset of the Fig. S1B where the absorbance at 325 nm is reported corrected for the dilution. The observed spectral variation is due to the deprotonation of the H_3L^+ species to form the H_2L one. These two species appear spectrally not well distinguishable. Increasing the pH till 8.8, the intensity of the peaks at 325 and 257 nm decreases while two new peaks appear at 378 nm and 266 nm due to the formation of the HL^- species. Four isosbestic points are present at 340, 300, 265 and 247 nm. At pH higher than 8.8, the intensity of the peak at 378 raises while that of the peak at 265 diminishes and a shoulder if formed at ≈ 300 nm, for the formation of the L^{2-} species. Two isosbestic point are present at 283 and 259 nm. Selected spectra at specific pH values are reported in Fig. S1; Compound **1b**: the analysis of the spectra recorded during the titration of **1b**, gives evidence of three equilibria (Fig. S2). At acidic pH two peaks are present at 252 and 325 nm. Increasing the pH till 8, the intensity of these two peaks decreases, while two new peaks appear at 264 and 378 nm. Four isosbestic points are present at 342, 292, 265 and 245 nm. After pH 8, the maximum of intensity shifts at 380 nm and three isosbestic points are present at 342, 292 and 265 nm. After pH 9, the peaks shift at 374 nm with larger width, a poor resolved isosbestic point is present at 332 nm. Selected spectra at specific pH values are reported in Fig. S2

1a, **1b**, **1d**, **1f**, and four for **1c** and **1e**. Some spectra recorded during the potentiometric titrations at different pH ranges are reported in Figs. S1–S6. A detailed description of the spectral variations for **1a** and **1b** is reported in Fig. 1 caption as an example, while and for **1c**–**1f** reported in the Supporting Fig. S7.

Calculation of the protonation constants

From the eigenvalue analysis of the spectrophotometric data, significant eigenvalues, interpreted as the number of linearly independent absorbing species were found (Malinowski 2002). The concentration profile as a function of pH and the pure UV–Vis spectra of all the absorbing species were then calculated without model assumptions. The results are shown in Fig. 2 for **1c** and in Figs. S1–6 E and S1–6 F for all the compounds.

Three significant eigenvalues were found for **1a**, four for **1b**, **1d** and **1f**, and five for **1c** and **1e**. Four eigenvalues were expected for **1a** and **1b** and five for the other compounds. Any attempt to fit the experimental data considering four eigenvalues for **1a** or five for **1d** and **1f** led to negative calculated pure spectra. These results showed that H_3L^+ and H_2L species for **1a** and H_4L^+ and H_3L species for **1d** and **1f** were not spectrally distinguishable. The potentiometric and spectrophotometric data were fitted simultaneously supposing a model considering three protonation equilibria (from L^{2-} to H_2L) for **1a** and **1b**, and four protonation equilibria (from L^{3-} to H_4L^+) for **1c**, **1d**, **1e**, and **1f**. The protonation constants and the refined pure spectra were calculated. The protonation constants are reported in Table 1. The pK values related to the formation of the H_3L^+ and H_4L^{2+} species for **1a** and **1f**, respectively, were outside the experimental pH range.

Table 1 Protonation constants of compounds **1a–f** at 25 °C and 0.1 M NaCl ionic strength

Compound	Species	Log β	pK
Overall stability constants			
1a	HL^-	10.2 (1)	10.2
	H_2L	18.30 (5)	8.1
	H_3L^+	19.8 (2)	< 2
1b	HL^-	9.40 (2)	9.4
	H_2L	18.2 (1)	8.8
	H_3L^+	21.5 (1)	3.3
1c	HL^{2-}	10.14 (1)	10.14
	H_2L^-	18.72 (1)	8.58
	H_3L	26.72 (1)	8.00
	H_4L^+	29.80 (4)	3.08
1d	HL^{2-}	11.0 (5)	11.0
	H_2L^-	20.3 (1)	9.3
	H_3L	27.8 (1)	7.5
	H_4L^+	28.5 (5)	< 2
1e	HL^-	9.81 (3)	9.81
	H_2L	18.52 (3)	8.71
	H_3L^+	26.09 (4)	7.57
	H_4L^{2+}	28.2 (4)	≈ 2
1f	HL^-	10.7 (2)	10.7
	H_2L	20.15 (2)	9.45
	H_3L^+	27.33 (2)	7.18
	H_4L^{2+}	29.3 (3)	< 2

The assignment of the protonation sequence was straightforward for compounds **1a** and **1b**. In fact, the first pK was related to the protonation of the phenolic oxygen atom, the second one to the iminic nitrogen, and the third one to the carboxylate group. To define the order in which the functional groups of **1c** were protonated, the absorptivity spectra

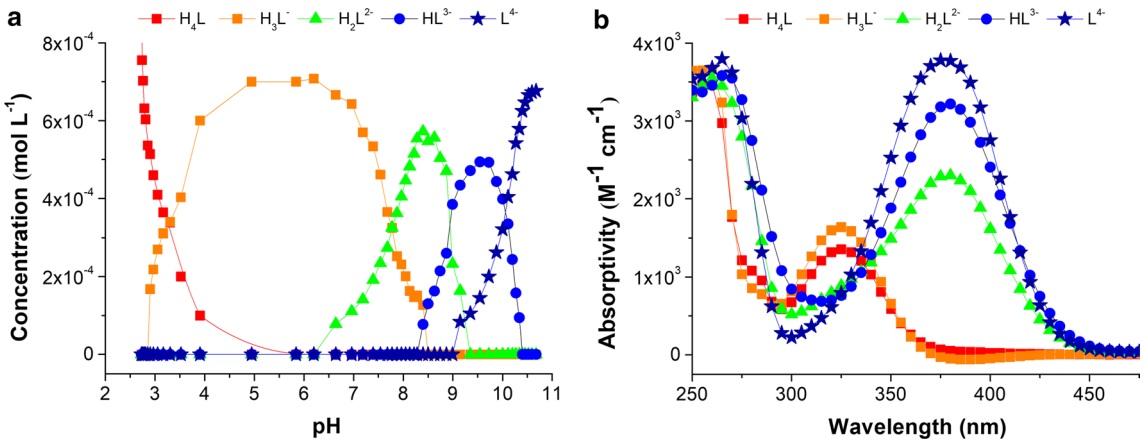

Fig. 2 Model free concentration profile (**a**) and pure spectra (**b**), calculated with eigenvalues analysis of the spectrophotometric data collected during the potentiometric titration of compound **1c** (7.07×10^{-4} M, 25 °C, 0.1 M NaCl, 1 cm optical path length, 25 °C)

of the different species of **1c** were compared with those of **1a**. The spectra of the HL species (charges are omitted for simplicity) of **1a** and **1c** were similar for the position and absorptivity ratio of the bands. This suggests that the same group was protonated in both species, i.e. the phenolic oxygen. The spectrum of the H_2L species of **1c** was different from that of the H_2L species of **1a**, where the iminic group was protonated, and was similar to that of the HL species of **1a**, where the iminic group is still not protonated. Then the second protonation in **1c** involves the sulfur atom. The spectra of the H_3L species of **1c** and that of the H_2L species of **1a** being similar, it can be deduced that the third protonation in **1c** involves the nitrogen atom. Finally, the fourth protonation occurs on the carboxylate group of **1c** (see Supporting, Scheme S1). For **1d**, by comparing the pure spectra of all the species formed by the studied compounds, the protonation involves in the order: the oxygen of the side chain, the phenolic oxygen, the imino group and lastly the carboxylate group (Scheme S2). For compound **1e**, considering the absorptivity spectra of the formed species and the pK 12.48 of the $–NH_2$ group in the arginine side chain (Yoo and Cui 2008), the first protonation appears to involve the $–NH_2$ group. The second protonation involves the phenolic oxygen, the third one the C=N group and the last one the carboxylate group. As regards compound **1f**, comparing the spectra of the absorbing species of all the studied compounds, and considering the protonation constants of histidine (Canel et al. 2006), the protonation involves in the order: the phenolic oxygen, the histidine nitrogen atom, the imino group and finally the carboxylate group (Scheme S3).

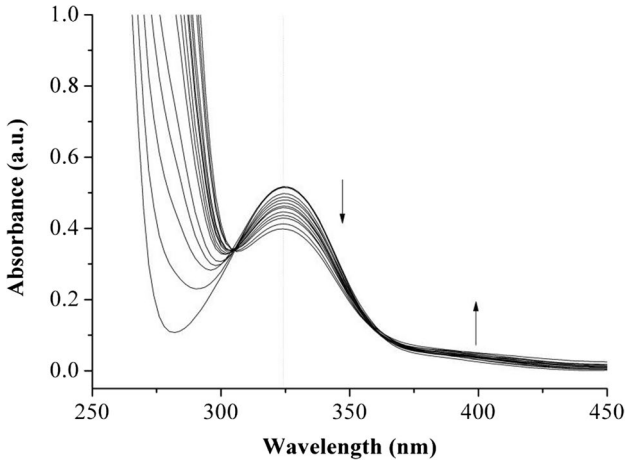

Fig. 3 Selected spectra recorded during the titration of 2×10^{-4} mmol of **1e** with 0.002 M ct-DNA; 0.01 M PIPES buffer, 25 °C, 1 cm optical path length. The arrows show the absorbance changes occurred during the titration

Table 2 DNA-binding constants of **1a–f**

Compound	K_b (M^{-1})
1a	48 (7)
1b	69 (8)
1c	229 (22)
1d	110 (12)
1e	148 (15)
1f	447 (39)

DNA binding study

The ability of compounds **1a–f** to bind DNA has been studied by UV–Vis titration with ct-DNA. The interaction of a molecule with DNA is known to result in a modification of its UV–Vis spectrum. The type of changes (red or blue shift, and hyper- or hypochromism) gives information on the binding mode (Babu et al. 2007). All the studied compounds showed, in the chosen experimental conditions, a peak at ≈ 325 nm. After each addition of DNA, the band decreased in intensity for compounds **1b–f**, whereas for the compound **1a** only slight variations of the absorbance were observed. No significant shift of the maximum was observed. The formation of another small band around 400 nm was also observed for all the compounds. Selected spectra collected during the titrations with ct-DNA are reported in Fig. 3 for **1e**, and in Fig. S8 for the other compounds. The spectral evidences suggest that compounds **1b–f** slightly interact with DNA thorough intercalation between base pairs.

The equilibrium reaction involved in DNA binding is described by the equation ($L + D \leftrightarrow LD$), where L is a generic molecule interacting with DNA, D is the DNA and LD is the formed adduct. The DNA binding constants, defined as $K_b = [LD]/[L][D]$, have been calculated by fitting the experimental absorbance data supposing the formation of the 1:1 compound-DNA adduct, according to Pivetta (Pivetta et al. 2014, 2017). The K_b values range from 48 to 447 (Table 2) and vary along the series **1f** > **1c** > **1e** > **1d** > **1b** > **1a**.

The affinity with the DNA appears related to the substituents present in the side chain. In fact, the lowest values (48 and 69 M^{-1}) were observed for **1a** and **1b**, bearing a methyl and an *iso*-propyl as substituents. The presence in the side-chain of the imidazole or the thiol group increased the K_b by ≈ 10 and ≈ 5 times, respectively, with respect to the compound **1a**. The measured K_b values were lower than those reported in literature for similar Schiff bases (Ali et al. 2014; Gowri and Jayabalakrishnan 2012; Arshad et al. 2014). The difference was probably due to the presence of other substituents participating in the DNA interaction. The experimental evidences showed that the amino acid moiety present in our compounds contributes, but not heavily, to the DNA binding.

Cytotoxicity

An evaluation of the cytotoxic activity of the synthetized compounds wasn carried out to study the influence of the introduction of the phenolic ring on the cytotoxicity of the amino acids. In fact, phenolic compounds are known to be toxic due to reactive oxygen species (ROS) formation (Michalowicz and Duda 2007). The antiproliferative activities of the six studied compounds were tested against three human solid tumor cell lines (lung squamous carcinoma (SK-MES-1), prostate carcinoma (DU-145), and hepatocellular carcinoma (Hep-G2)), and two human haematological tumor cell lines (acute T-lymphoblastic leukemia (CCRF-CEM), and acute B-lymphoblastic leukemia (CCRF-SB)). All the studied compounds showed IC50 values higher than 100 µM against all the tested tumor cell lines (Tables 3, 4) and were then devoid of a significant cytotoxic activity (Fig. 4a–e).

Conclusions

The Schiff bases **1a–f** were synthesized and characterized by means of elemental analysis, NMR and IR spectroscopy. The protonation and DNA-binding constants, and the cytotoxic activity were determined. With respect to the literature methods, reduced reaction time (for **1c** and **1d**), double amount of salicylaldehyde (for **1f**) and sodium sulfate addition (for **1a** and **1b**) were needed for a better yield. All compounds were obtained as a mixture of E and Z geometric isomers, the E isomer always being more abundant. The protonation of the carboxylate group happens at around pH 3 for **1b** and **1c**, whereas for all the other compounds around 2 or lower. The protonation of the imino group occurs between pH 7.18 and 8.8, while that of the phenolic oxygen between pH 8.71 and 10.7. The protonation of the amino acid side chain occurs before the protonation of the phenolic oxygen only for **1d** and **1e**. In all compounds the imino group is protonated after the carboxylic group. The examined compounds do not show cytotoxic activity, despite the presence of the phenolic ring derived from salicylaldehyde. Nevertheless, **1a–f** show DNA binding constant in the 48–447 M^{-1} range. The absence of cytotoxicity and the poor reactivity with DNA, confirm the feasibility of these compounds for pharmaceutical applications, also in metal complexes, to exploit their unique properties. In fact, although the ligands are devoid of significant activity, an antitumor activity of their metal complexes is not totally unexpected. As an additional interesting application, the studied compounds may be also promising green catalysts in chiral synthesis, due to their intrinsic chirality derived from the L-amino acid moiety.

Table 3 Antiproliferative activity in vitro of the synthesised compounds against human leukaemia-/lymphoma-derived cell lines

Compounds	IC_{50} (µM)[a]	
	CCRF-CEM[b]	CCRF-SB[c]
1a		
1b	> 100	> 100
1c	> 100	> 100
1d	> 100	> 100
1e	> 100	> 100
1f	> 100	> 100
Ref. compd		
VINCRISTINE	0.0007	0.0009

[a]Compound concentration required to reduce cell proliferation by 50%, as determined by the MTT method, under conditions allowing untreated controls to undergo at least three consecutive rounds of multiplication

[b]Human acute T-lymphoblastic leukaemia

[c]Human acute B-lymphoblastic leukaemia; vincristine was used as a reference antitumor compound

Table 4 Antiproliferative activity in vitro of Schiff bases compounds against solid tumour-derived (SK-ME 1, DU 145, HEP-G2) cell lines

Compounds	[a]IC_{50} (µM)		
	[b]SK-MES 1	[c]DU 145	[d]HEP-G2
1a	> 100	> 100	> 100
1b	> 100	> 100	> 100
1c	> 100	> 100	> 100
1d	> 100	> 100	> 100
1e	> 100	> 100	> 100
1f	> 100	> 100	> 100
Ref. compd			
VINCRISTINE	0.17	1.18	0.005

[a]Compound concentration (µM) required to reduce cell proliferation by 50%, as determined by the MTT method, under conditions allowing untreated controls to undergo at least three consecutive rounds of multiplication

[b]Human lung squamous carcinoma

[c]Human prostate carcinoma

[d]Human hepatocellular carcinoma; vincristine was used as a reference antitumor compound

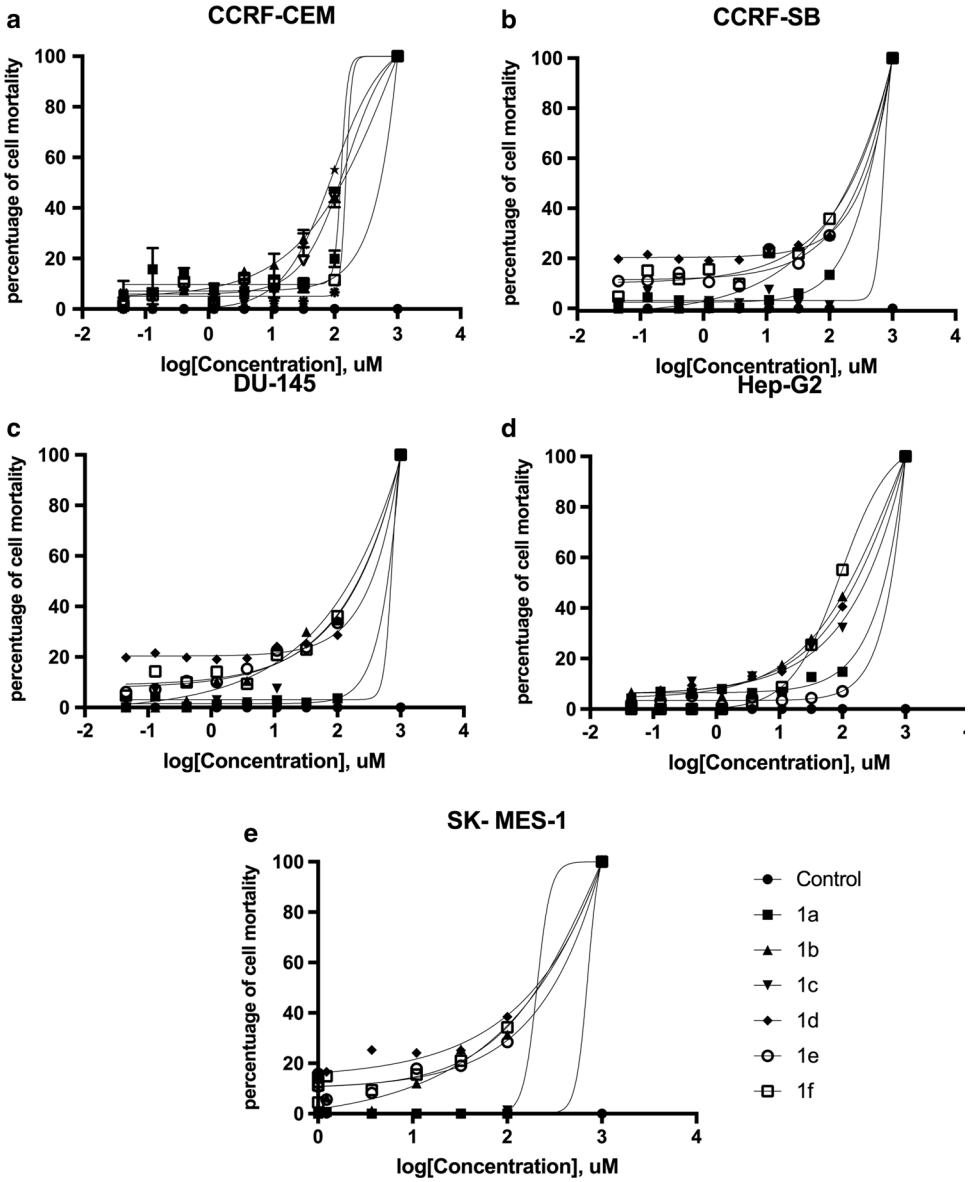

Fig. 4 Dose response of antiproliferative activity of the studied compounds (**1a**–**1f**) against human leukemia- cell lines CCRF-CEM (**a**), CCRF-SB (**b**) and solid tumor cell lines DU-145 (**c**), Hep-G2 (**d**) and SK-MES-1 (**e**). The cell lines were incubated with different concentrations (0.045 µM, 0.13 µM, 0.41 µM, 1.23 µM, 3.7 µM, 11 µM, 33 µM, 100 µM, 1000 µM) of each tested compound for 72 h

Compliance with ethical standards

Conflict of interest The authors declare no conflicts of interest.

Ethical approval This article does not contain any studies with human participants or animals performed by any of the authors.

References

Ali AQ, Teoh SG, Salhin A, Eltayeb NE, Khadeer Ahamed MB, Abdul Majid AM (2014) Synthesis of isatin thiosemicarbazones derivatives: in vitro anti-cancer, DNA binding and cleavage activities. Spectrochim Acta A Mol Biomol Spectrosc 125:440–448. https://doi.org/10.1016/j.saa.2014.01.086

Antony R, Arun T, Manickam STD (2019) A review on applications of chitosan-based Schiff bases. Int J Biol Macromol 129:615–633. https://doi.org/10.1016/j.ijbiomac.2019.02.047

Arshad N, Ahmad M, Ashraf MZ, Nadeem H (2014) Spectroscopic, electrochemical DNA binding and in vivo anti-inflammatory studies on newly synthesized Schiff bases of 4-aminophenazone. J Photochem Photobiol B Biol 138:331–346. https://doi.org/10.1016/j.jphotobiol.2014.06.014

Babu MSS, Reddy KH, Krishna PG (2007) Synthesis, characterization, DNA interaction and cleavage activity of new mixed ligand copper(II) complexes with heterocyclic bases. Polyhedron 26:572–580. https://doi.org/10.1016/j.poly.2006.08.026

Banti CN, Hadjikakou SK, Sismanoglu T, Hadjiliadis N (2019) Anti-proliferative and antitumor activity of organotin(IV) compounds. An overview of the last decade and future perspectives. J Inorg Biochem 194:114–152

Canel E, Gültepe A, Doğan A, Kılıç E (2006) The determination of protonation constants of some amino acids and their esters by potentiometry in different media. J Solut Chem 35:5–19. https://doi.org/10.1007/s10953-006-8934-3

Chow MJ, Licona C, Wong DYQ, Pastorin G, Gaiddon C, Ang WH (2014) Discovery and investigation of anticancer ruthenium–arene Schiff-base complexes via water-promoted combinatorial three-component assembly. J Med Chem 57:6043–6059. https://doi.org/10.1021/jm500455p

Dalapati S, Jana S, Guchhait N (2014) Anion recognition by simple chromogenic and chromo-fluorogenic salicylidene Schiff base or reduced-Schiff base receptors. Spectrochim Acta Part A Mol Biomol Spectrosc 129:499–508. https://doi.org/10.1016/j.saa.2014.03.090

Dossetter AG, Jamison TF, Jacobsen EN (1999) Highly enantio- and diastereoselective hetero-Diels-Alder reactions catalyzed by new chiral tridentate chromium (III) catalysts. Angew Chem Int Ed Engl 38:2398–2400. https://doi.org/10.1002/(sici)1521-3773(19990816)38:16%3c2398:aid-anie2398%3e3.0.co;2-e

El-Sherif AA, Aljahdali MS (2013) Review: protonation, complex-formation equilibria, and metal–ligand interaction of salicylaldehyde Schiff bases. J Coord Chem 66:3423–3468. https://doi.org/10.1080/00958972.2013.839027

Ershov AY, Nasledov DG, Nasonova KV, Sezyavina KV, Susarova TV, Lagoda IV, Shamanin VV (2013) Ring-chain tautomerism of 2-aryl-6-oxohexahydropyrimidine-4-carboxylic acid sodium salts. Chem Heterocycl Compd 49:640–645. https://doi.org/10.1007/s10593-013-1287-0

Galić N, Cimerman Z, Tomišić V (1997) Tautomeric and protonation equilibria of Schiff bases of salicylaldehyde with aminopyridines. Anal Chim Acta 343:135–143. https://doi.org/10.1016/S0003-2670(96)00586-7

Gans P, O'Sullivan B (2000) GLEE, a new computer program for glass electrode calibration. Talanta 51:33–37. https://doi.org/10.1016/s0039-9140(99)00245-3

Gans P, Sabatini A, Vacca A (1996) Investigation of equilibria in solution. Determination of equilibrium constants with the hyperquad suite of programs. Talanta 43:1739–1753. https://doi.org/10.1016/0039-9140(96)01958-3

Gomes LMF, Vieira RP, Jones MR, Wang MCP, Dyrager C, Souza-Fagundes EM et al (2014) 8-Hydroxyquinoline Schiff-base compounds as antioxidants and modulators of copper-mediated Aβ peptide aggregation. J Inorg Biochem 139:106–116. https://doi.org/10.1016/j.jinorgbio.2014.04.011

Gowri M, Jayabalakrishnan C (2012) DNA binding and cytotoxicity of newly synthesized Schiff base (Z)-4-(((2-hydroxyphenyl)amino)(phenyl)methylene)-3-methyl-1-phenyl-1H-pyrazol-5(4H)-one and its analogues. Int J Appl Biol Pharm Technol 3:327–337

Gran G (1952) Determination of the equivalence point in potentiometric titrations-Part II. Analyst 77:771

Hiskey RG, Jung JM (1963) Azomethine chemistry. II. Formation of peptides from oxazolidine-5-ones. J Am Chem Soc 85:578–582. https://doi.org/10.1021/ja00888a021

Hsieh SH, Kuo YP, Gau HM (2007) Synthesis, characterization, and structures of oxovanadium(V) complexes of Schiff bases of beta-amino alcohols as tunable catalysts for the asymmetric oxidation of organic sulfides and asymmetric alkynylation of aldehydes. Dalton Trans. https://doi.org/10.1039/b613212j

Latt SA, Stetten G, Juergens LA, Willard HF, Scher CD (1975) Recent developments in the detection of deoxyribonucleic acid synthesis by 33258 Hoechst fluorescence. J Histochem Cytochem 23:493–505. https://doi.org/10.1177/23.7.1095650

Liu X, Manzur C, Novoa N, Celedón S, Carrillo D, Hamon JR (2018) Multidentate unsymmetrically-substituted Schiff bases and their metal complexes: synthesis, functional materials properties, and applications to catalysis. Coord Chem Rev 357:144–172

Liu S, Peng J, Yang H, Bai Y, Li J, Lai G (2012) Highly efficient and convenient asymmetric hydrosilylation of ketones catalyzed with zinc Schiff base complexes. Tetrahedron 68:1371–1375. https://doi.org/10.1016/j.tet.2011.12.054

Malik MA, Dar OA, Gull P, Wani MY, Hashmi AA (2018) Heterocyclic Schiff base transition metal complexes in antimicrobial and anticancer chemotherapy. Med Chem Commun 9:409–436. https://doi.org/10.1039/c7md00526a

Malinowski ER (2002) Factor analysis in chemistry, 3rd edn. Wiley, New York

Maurya MR, Kumar U, Correia I, Adão P, Costa Pessoa J (2008) A polymer-bound oxidovanadium(IV) complex prepared from an L-cysteine-derived ligand for the oxidative amination of styrene. Eur J Inorg Chem. https://doi.org/10.1002/ejic.200700662

Metzler CM, Cahill A, Metzler DE (1980) Equilibria and absorption spectra of Schiff bases. J Am Chem Soc 102:6075–6082. https://doi.org/10.1021/ja00539a017

Michałowicz J, Duda W (2007) Phenols-sources and toxicity. Polish J Environ Stud 16:347–362

Murmur J (1961) A procedure for the isolation of deoxyribonucleic acid from micro-organisms. J Mol Biol 3:208–218. https://doi.org/10.1016/S0022-2836(61)80047-8

Palomo C, Aizpurua JM, Ganboa I, Oiarbide M (1999) Asymmetric synthesis of β-lactams by Staudinger Ketene-imine cycloaddition reaction. Eur J Org Chem. https://doi.org/10.1002/(SICI)1099-0690(199912)1999:12%3c3223:AID-EJOC3223%3e3.0.CO;2-1

Pauwels R, Balzarini J, Baba M, Snoeck R, Schols D, Herdewijn P et al (1988) Rapid and automated tetrazolium-based colorimetric assay for the detection of anti-HIV compounds. J Virol Methods 20:309–321. https://doi.org/10.1016/0166-0934(88)90134-6

Pessoa JC, Mannar MR (2017) Vanadium complexes supported on organic polymers as sustainable systems for catalytic oxidations. Inorg Chim Acta 455:415–428

Pillai MRA, Kothari K, Banerjee S, Samuel G, Suresh M, Sarma HD, Jurisson S (1999) Radiochemical studies of 99mTc complexes of modified cysteine ligands and bifunctional chelating agents. Nucl Med Biol 26:555–561

Pivetta T, Trudu F, Valletta E, Isaia F, Castellano C, Demartin F et al (2014) Novel copper(II) complexes as new promising antitumour agents. A crystal structure of [Cu(1,10-phenanthroline-5,6-dione)2(OH_2)($OClO_3$)](ClO_4). J Inorg Biochem 141:103–113. https://doi.org/10.1016/j.jinorgbio.2014.08.011

Pivetta T, Valletta E, Ferino G, Isaia F, Pani A, Vascellari S, Castellano C, Demartin F, Cabiddu MG, Cadoni E (2017) Novel coumarins and related copper complexes with biological activity: DNA binding, molecular docking and in vitro antiproliferative activity. J Inorg Biochem 177:101–109. https://doi.org/10.1016/j.jinorgbio.2017.09.013

Qiao X, Ma ZY, Xie CZ, Xue F, Zhang YW, Xu JY et al (2011) Study on potential antitumor mechanism of a novel Schiff base copper(II) complex: synthesis, crystal structure, DNA binding, cytotoxicity and apoptosis induction activity. J Inorg Biochem 105:728–737. https://doi.org/10.1016/j.jinorgbio.2011.01.004

Qin W, Long S, Panunzio M, Biondi S (2013) Schiff bases: a short survey on an evergreen chemistry tool. Molecules 18:12264–12289. https://doi.org/10.3390/molecules181012264

Rajesh CM, Ray M (2014) Characterization of a meso-chiral isomer of a hexanuclear Cu(II) cage from racemization of the L-alanine Schiff base. Dalton Trans 43:12952–12960. https://doi.org/10.1039/c4dt01443j

Rao G, Philipp M (1991) Boronic acid catalyzed hydrolyses of salicylaldehyde imines. J Org Chem 56:1505–1512. https://doi.org/10.1021/jo00004a031

Reichmann ME, Rice SA, Thomas CA, Doty P (1954) A further examination of the molecular weight and size of desoxypentose nucleic

acid. J Am Chem Soc 76:3047–3053. https://doi.org/10.1021/ja01640a067

Saleem H, Erdogdu Y, Subashchandrabose S, Thanikachalam V, Jayabharathi J, Ramesh Babu N (2012) Structural and vibrational studies on (E)-2-(2-hydroxybenzylidenamino)-3-phenylpropionic acid using experimental and DFT methods. J Mol Struct 1030:157–167. https://doi.org/10.1016/j.molstruc.2012.04.011

Smith HE, Burrows EP, Marks MJ, Lynch RD, Chen FM (1977) Optically active amines. 22. Application of the salicylidenimino chirality rule to α-amino acids. J Am Chem Soc 2:707–713. https://doi.org/10.1021/ja00445a008

Turan B, Şendil K, Şengül E, Gültekin MS, Taslimi P, Gulcin I, Supuran CT (2016) The synthesis of some β-lactams and investigation of their metal-chelating activity, carbonic anhydrase and acetylcholinesterase inhibition profiles. J Enzyme Inhib Med Chem 31 (sup1):79–88

Türkoğlu G, Berber H, Dal H, Öğretir C (2011) Synthesis, characterization, tautomerism and theoretical study of some new Schiff base derivatives. Spectrochim Acta A Mol Biomol Spectrosc 79:1573–1583. https://doi.org/10.1016/j.saa.2011.04.089

Vilanova B, Gallardo J, Caldés C, Adrover M, Ortega-Castro J, Muñoz F et al (2012) Formation of Schiff bases of O-phosphorylethanolamine and O-phospho-d, l-serine with pyridoxal 5′-phosphate. Experimental and theoretical studies. J Phys Chem A 116:1897–1905. https://doi.org/10.1021/jp2116033

Yang ZY, Yang RD, Li FS, Yu KB (2000) Crystal structure and antitumor activity of some rare earth metal complexes with Schiff base. Polyhedron 19:2599–2604. https://doi.org/10.1016/S0277-5387(00)00562-3

Yoo J, Cui Q (2008) Does arginine remain protonated in the lipid membrane? Insights from microscopic pKa calculations. Biophys J Biophys Lett 94:L61–63. https://doi.org/10.1529/biophysj.107.122945

Zhang N, Fan Y, Zhang Z, Zuo J, Zhang P, Wang Q et al (2012) Syntheses, crystal structures and anticancer activities of three novel transition metal complexes with Schiff base derived from 2-acetylpyridine and l-tryptophan. Inorg Chem Commun 22:68–72. https://doi.org/10.1016/j.inoche.2012.05.022

Zhong X, Yi J, Sun J, Wei HL, Liu WS, Yu KB (2006) Synthesis and crystal structure of some transition metal complexes with a novel bis-Schiff base ligand and their antitumor activities. Eur J Med Chem 41:1090–1092. https://doi.org/10.1016/j.ejmech.2006.05.009